Surface contributions to the effective optical properties of porous silicon

J.E. Lugo[a], J.A. del Río[b], J. Tagüeña-Martínez[b],*

[a] *Facultad de Ciencias, Universidad Autónoma del Estado de Morelos, 62210 Cuernavaca, Morelos, Mexico*
[b] *Laboratorio de Energía Solar, IIM-UNAM A.P. 34, Temixco, 62580 Morelos, Mexico*

Abstract

Porous silicon (PS) presents efficient photoluminescence and electroluminescence with potential applications in the optoelectronic industry, in particular in photovoltaic devices. It is now generally accepted that the interesting optical properties of PS are due to two combined aspects: on the one hand, the quantum confinement and on the other, the surface states. Although there has been a great effort to study PS, its transport properties are still not well understood. Due to the complex structure of PS an averaging theory to describe its effective properties is justified. In this work the effective dielectric function, effective absorption coefficient and effective refractive index are calculated using the volume averaging method for a model of periodic columns with different surface coatings simulating porous silicon. This approach allows analytical results within certain approximations and the analysis of surface contributions. The method uses parameters to characterize the bulk and the surface. We choose for the bulk c-Si, and cover it with three different possible surfaces: siloxane, a-Si : H and SiO_2. The results are compared with experimental data and other theoretical approaches for silicon wires. We obtain good agreement with some experimental results showing the important role of the surface in the effective response of porous silicon. © 1998 Elsevier Science B.V. All rights reserved.

Keywords: Porous silicon; Optical properties; Surface states

---

* Corresponding author.

1. Introduction

Human skill to build new materials from the around one hundred elements in nature is amazing and, from new materials, new technologies and applications develop. In particular, the growth of nanocomposite materials is having considerable impact on physics. These structures which are on an intermediate scale between the small molecules, traditionally studied by quantum chemists, and the crystalline solids, studied by solid state physicists, exhibit qualitatively new phenomena. This revolution in material science is somehow similar to the one due to the use and study of amorphous and disordered materials. Porous silicon (PS) has both features: it is a disordered nanostructure which presents efficient photoluminiscence and electroluminescence, and has potential applications in optoelectronic devices [1,2]. Its possible application has stimulated the research in photodetectors [3,4], silicon-based LED [5] and solar cells of PS on c-Si [6,7].

PS can be grown starting from crystalline silicon c-Si [8] by means of an electrochemical dissolution in hydrofluoric acid. Such reaction originates pores in the c-Si, and the new material presents an efficient luminescence at room temperature [9]. It has been observed that the properties of PS depend on the acid concentration, the current intensity and the concentration and type of the dopants of the crystalline substrate [10]. There have been many experimental efforts to characterize the structure of PS using a great variety of techniques. Scanning electron microscope studies have revealed a structure of coral-like columns [11], where the columns have diameters of the order of nanometers and heights of microns. The surface of the silicon columns is passivated, mainly with hydrogen. One could say that the PS is formed of c-Si in the bulk, some compound of silicon with hydrogen or oxygen with a certain degree of amorphicity on the surface and air surrounding the columns.

From the theoretical point of view, an interesting debate was originated with regard to the mechanism that produces the luminescence in PS. It can be explained using a quantum confinement argument [9], but it can also be attributed to surface states [12], for instance, interfacial oxide-related defects [13]. First principles calculations in quantum wires of silicon indicate that the band gap energy increases and becomes direct [14], giving a possible confinement explanation for the optical properties of PS. However, it has been experimentally seen that PS has an indirect band gap [15]. On the other hand, the surface effects cannot be ignored. For example, the efficiency of the luminescence in PS is linked with the surface passivation with hydrogen and aging changes the luminescence of the samples. While the red luminescence could be explained by means of quantum confinement, the blue luminescence has been related experimentally to the oxidation of the surface [16]. Therefore, in order to describe the optical properties of PS it is necessary to develop a theoretical framework that considers not only the bulk but also the surface contributions.

As we have already mentioned, besides being photoluminescent, PS also exhibits electroluminescence. Its conductivity is very difficult to measure because PS is a very fragile material. There are some results that indicate that PS presents high resistivity [6,17–19]. This last property has suggested that it is a suitable candidate to manufacture c-Si insulator structures, which are very important in the minimization of electric

losses in solar cells and in the microelectronics industry [8]. In order to avoid optical reflection in solar cells, PS could also be used as an antireflection layer.

For all these applications it is important to model the effective optical properties of PS. In previous works we have calculated its effective conductivity properties including surface contributions [18–22]. There are already some theoretical approaches to the effective dielectric function of PS [23,24] and the effective absorption coefficient [25], but neither of them studied the role of surface effects specifically.

Here, we have calculated some effective optical properties: the effective dielectric function, the effective absorption coefficient and the effective refractive index for a periodic arrangement of columns of c-Si, using a classical approach: the theorem of the volume averaging method (VAM) [26]. It averages point transport equations over a volume whose radius is much larger than the characteristic length of the microstructure, but much smaller than the macroscopic scale. This effective theory includes in an easy way the surface effects through the theorem of the surface average [27]. The average transport equations are written in terms of effective parameters, which include the physical properties of the components and the specific geometry of the microstructure.

In the next section we present the model and the method to calculate the axial and transverse components of the effective dielectric function and, from it, the effective absorption coefficient of PS, using the Chang approximation [18] and the long wavelength limit in order to obtain analytical results. We present our results modeling PS as a bundle of c-Si cylindrical columns coated with different materials. We analyze the effects of a-Si : H, siloxane and SiO_2 coverages in the optoelectronic properties of this model. Finally, we close the paper with some remarks and conclusions.

2. The model and the method

The simplest possible geometry is to consider porous silicon as a periodic network of parallel columns in square cells (see Fig. 1). These columns are composed in their bulk by crystalline silicon and on their surface, for instance, by hydrogenated amorphous silicon or siloxane thin films. PS has clearly two bulk components, namely silicon and air.

In our geometrical model a change of porosity means a change in the width of the columns. The periodic model of circles in squares has a percolation limit when the porosity is approximately 21%, while it has been observed that the luminescence appears at higher porosities such as 50%. This suggests the use of a periodic model of square parallel columns with a unitary square cell, where percolation occurs at a porosity of the order at 50%. However, for high porosities, the best choice is a geometrical model known as the cell of Chang [29], which consists of a periodic arrangement of parallel cylinders with a unitary circular cell. In this model the limit of percolation is never attained and therefore it is only valid for high porosities, which is the case in efficient luminescent PS samples. In the Chang cell we need the following
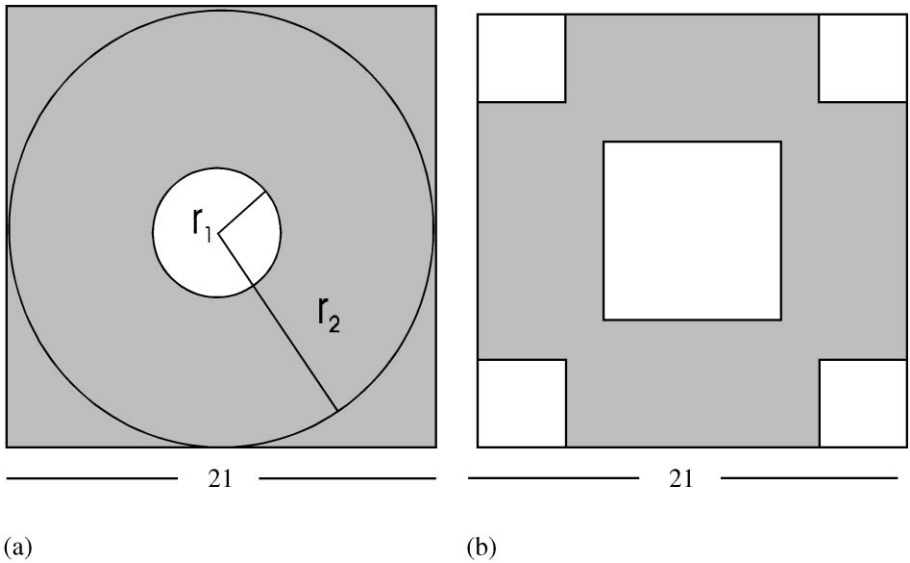
Fig. 1. Geometrical model for porous silicon: (a) square parallel columns in a periodic network with a unit cell of length $2l$ and (b) parallel cylinders in a periodic network with a unit cell of length $2l$ and the Chang model.

geometrical parameters:

$$a_v = \frac{2(1-P)}{r_1}, \qquad r_1 = r_2\sqrt{(1-P)}, \tag{1}$$

where r_2 is the radio of the unitary circular cell, P is the porosity, a_v is the area per volume unit and r_1 is the radius of the column.

The local problem for the electromagnetic transport is given by the wave equation

$$\varepsilon_i \nabla^2 \varphi_i = -\frac{\omega^2 \varepsilon_i^2}{c^2}\varphi_i \quad i = 1,2, \tag{2}$$

with the boundary conditions

$$\hat{n}_{12}\cdot \varepsilon_1 \nabla\varphi_1 + \hat{n}_{21}\cdot \varepsilon_2 \nabla\varphi_2 = \rho_s^{\text{ext}},$$

$$\varphi_1 = \varphi_2 \quad \text{at } A^{12}, \tag{3}$$

where c is the speed of the light, ε_i is the dielectric function of the ith component, ρ_s^{ext} is the real surface charge density, ω is the frequency, φ_i is the electric potential of the ith component, $\hat{n}_{ij}$ is the unit normal vector pointing from the j component towards the i component and A^{ij} is the intercomponents' area. It is possible to demonstrate [27] that in the formalism of VAM, the first boundary condition is equivalent to

$$\hat{n}_{12}\cdot \varepsilon_1 \nabla\varphi_1 + \hat{n}_{21}\cdot \varepsilon_2 \nabla\varphi_2 = \varepsilon_s d \nabla_s^2 \varphi_s + \frac{\omega^2 \varepsilon_s^2 d}{c^2}\varphi_s = \rho_s^{\text{ext}}, \tag{4}$$

where d is the effective width of the surface, ε_s is the dielectric function in the intercomponents' region, φ_s is the electric potential on the surface and V_s is an operator of projection, defined as

$$V_s = (1 - \hat{n}_{12}\hat{n}_{12}) \cdot V, \tag{5}$$

where 1 is the unitary tensor and V is the gradient operator.

Using the relations of VAM [20] on Eq. (2) we obtain

$$[\varepsilon_1 f_1 + \varepsilon_2 f_2 + a_v \varepsilon_s d] V^2 \bar{\varphi} + \frac{1}{V} V \cdot \int_{A^{21}} [- \varepsilon_1 \tilde{\varphi}_1 + \varepsilon_2 \tilde{\varphi}_2 + 2\varepsilon_s dH \tilde{\varphi}_1] \hat{n}_{21} \, dA$$

$$= -\frac{\omega^2}{c^2} [\varepsilon_1^2 f_1 + \varepsilon_2^2 f_2 + a_v \varepsilon_s^2 d] \bar{\varphi}. \tag{6}$$

Here we have defined the local microscopic deviations of the electric potential $\tilde{\varphi}_i$ by

$$\varphi_i = f_i \langle \varphi_i \rangle^i + \tilde{\varphi}_i, \tag{7}$$

where $\bar{\varphi}$ is the effective electrical potential, f_i is the volume fraction of the ith-component, $a_v = A^{12}/V$ and H is the curvature of the intercomponents' region. Eq. (9) is not an effective medium equation, because it still contains terms with microscopic deviations defined in Eq. (7). At this point we need constitutive equations for $\tilde{\varphi}_i$. Following previous papers [20,27] our guess is

$$\tilde{\varphi}_i - \boldsymbol{g}_i \cdot V\bar{\varphi}, \quad i = 1,2, \tag{8}$$

$$\tilde{\varphi}_s - \boldsymbol{g}_i \cdot V\bar{\varphi} \quad \text{at} \quad A^{12}.$$

Substituting Eq. (8) in Eq. (6) we can obtain, in the long wave limit,

$$\varepsilon \colon VV\bar{\varphi} = -\frac{\omega^2}{c^2} [\varepsilon_1^2 f_1 + \varepsilon_2^2 f_2 + a_v \varepsilon_s^2 d] \bar{\varphi}, \tag{9}$$

where

$$\varepsilon = [\varepsilon_1 f_1 + \varepsilon_2 f_2 + a_v \varepsilon_s d] 1 + D, \tag{10}$$

$$D = \frac{1}{V} \int_{A^{21}} \hat{n}^{21} [- \varepsilon_1 + 2\varepsilon_s dH + \varepsilon_2] \boldsymbol{g}_1 \, dA,$$

with ε the effective dielectric tensor.

For the chosen geometry, due to symmetry considerations, only two terms in the effective dielectric tensor are significant. One is the axial term $\varepsilon_\parallel$ and the other is the transverse term $\varepsilon_\perp$, which can be expressed as

$$\varepsilon_\parallel = \hat{k} \cdot \boldsymbol{\varepsilon} \cdot \hat{k} = \varepsilon_1 f_1 + \varepsilon_2 f_2 + \varepsilon_s \, da_v \tag{11}$$

$$\varepsilon_\perp = \hat{i} \cdot \boldsymbol{\varepsilon} \cdot \hat{i} \cdot = \varepsilon_\parallel + \hat{i} \cdot D \cdot \hat{i}.$$

At this point, we can see explicitly the surface contribution in the case of the axial component of a cylindrical geometry. However, for the transverse component, we

need to calculate the specific expressions for microscopic fields g_1. An equation for g_1 can be obtained in a straightforward way [26,30], in dimensionless form as

$$\frac{1}{\xi}\frac{\partial}{\partial\xi}\left[\xi\frac{\partial G_{1x}}{\partial\xi}\right]+\frac{1}{\xi^2}\frac{\partial^2 G_{1x}}{\partial\theta^2}=0 \quad \text{with} \quad \xi=\frac{r}{r_2} \quad \text{and} \quad \theta\in[0,2\pi]$$

$$\frac{\partial G_{1x}}{\partial\xi}-\Delta\frac{\partial G_{2x}}{\partial\xi}-\left(\frac{r_2}{r_1}\right)\Lambda\frac{\partial^2 G_{1x}}{\partial\theta^2}=\cos\theta[-1-\Lambda+\Delta] \quad \text{at} \quad \xi=\frac{r_1}{r_2},$$

$$G_{1x}=G_{2x} \quad \text{at} \quad \xi=\frac{r_1}{r_2}, \tag{12}$$

$$G_{1x}\neq\infty \quad \text{at} \quad \xi=0,$$

$$G_{2x}=0 \quad \text{at} \quad \xi=1,$$

where $\Delta=\varepsilon_2/\varepsilon_1$, $\Lambda=\varepsilon_s d/\varepsilon_1 r_1$ and

$$G_{ix}=\frac{g_i\cdot\hat{i}}{r_2}. \tag{13}$$

The last two relations in Eq. (12) have two implications: first, the good behavior of the G_{1x} field at the origin and second, the spatially periodic boundary condition [28].

The solution in the representative cell (see Fig. 1) is given by

$$G_{1x}=-\frac{\xi\cos\theta}{\left[1+\dfrac{2\Delta}{P[1+\Lambda-\Delta]}\right]}. \tag{14}$$

Substituting in Eq. (11) we arrive at

$$\varepsilon_\perp=\varepsilon_\parallel+\varepsilon_1\left[\frac{(1-P)(-1-\Lambda+\Delta)}{(1+\delta)}\right], \tag{15}$$

where $\delta=2\Delta P[[1+\Lambda-\Delta]P]$ and P is the porosity.

It is important to verify that Eqs. (11) and (15) reproduce the limits previously calculated by other technique. Removing the contribution of the intercomponent region (neglecting surface effects, $\Lambda=0$) we recover the Maxwell–Garnett approximation.

For the calculation of the effective absorption coefficient, we use the well-known relationship

$$\alpha=\frac{\omega \, Im \, \varepsilon}{nc}, \tag{16}$$

where n is the effective refractive index, whose value is the real part of the square root of the effective dielectric function and $Im \, \varepsilon$ is the imaginary part of the effective dielectric function in a given direction (in our case axial or transverse).

3. Results

In order to calculate the effective dielectric function – Eq. (11) – for different porosities, we need to introduce experimental parameters for the components. There are available results for the energy-dependent dielectric function of for c-Si [31], a-Si : H [32], siloxane [33] and SiO_2 [34].

In the following, we analyze only the transverse component of the effective dielectric function which is the one measured experimentally. Fig. 2 shows the results for this normalized component in different cases: without skin and with siloxane, a-Si : H and SiO_2 coverages for $d = 10^{-10}$ m. Our results calculated for 70% porosity are compared with an experiment [35] done on a sample with this porosity, measured with the technique of reflection with normal incidence. For low energies, Koshida's results are in better agreement with the calculations in the absence of any skin. Apparently in the experiment the surface effects were removed, after oxidizing the sample, thus the experimental data cannot help us to evaluate the best coverage surface choice, but it is encouraging that they are consistent with an effective medium approach.

Our results do show that the surface has a "tuning" effect on the effective dielectric function and that this effect is more appreciable if on the surface instead of siloxane we place a-Si : H or SiO_2 on the surface. Furthermore, including the surface contribution in the calculation smooths the peaks observed experimentally at low energies in crystalline samples.
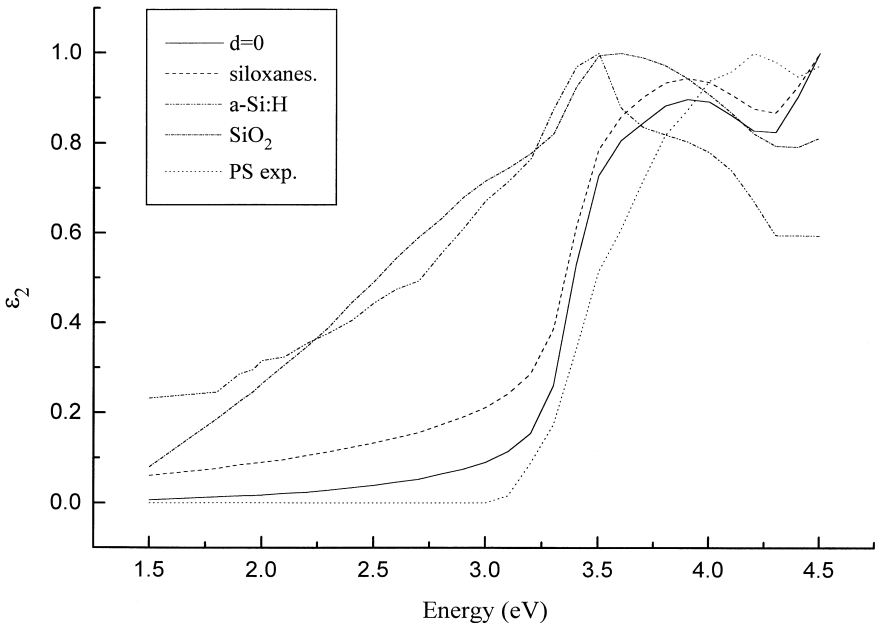

Fig. 2. Imaginary part of the normalized transverse component of the effective dielectric function of porous silicon without skin ($d = 0$ m) and with siloxane, a-Si : H and SiO_2 on the surface ($d = 10^{-10}$ m) compared with experimental results [35], at 70% of porosity.
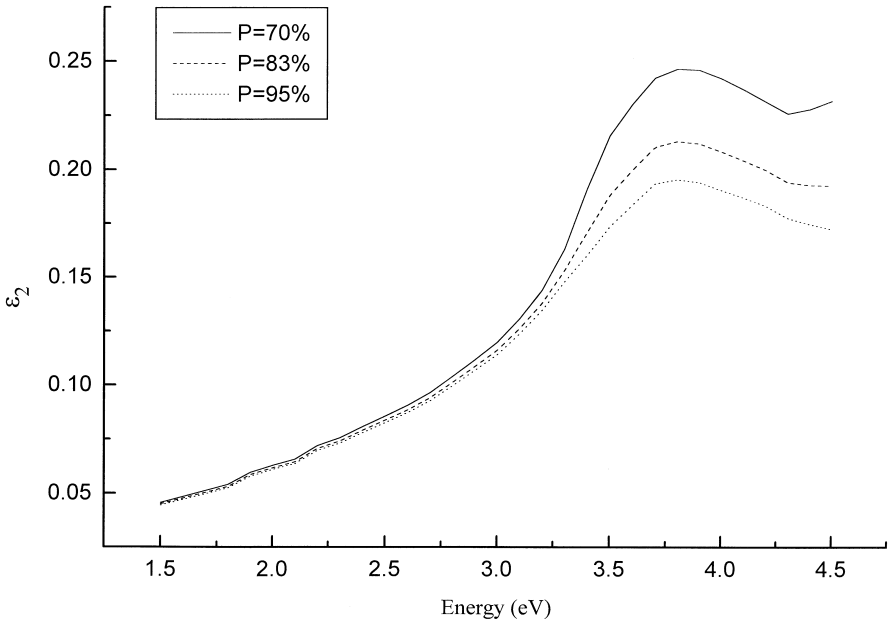
Fig. 3. Imaginary part of the transverse component of the effective dielectric function of porous silicon with siloxane on the surface and three different porosities 70%, 83% and 95%; $d = 10^{-9}$ m.
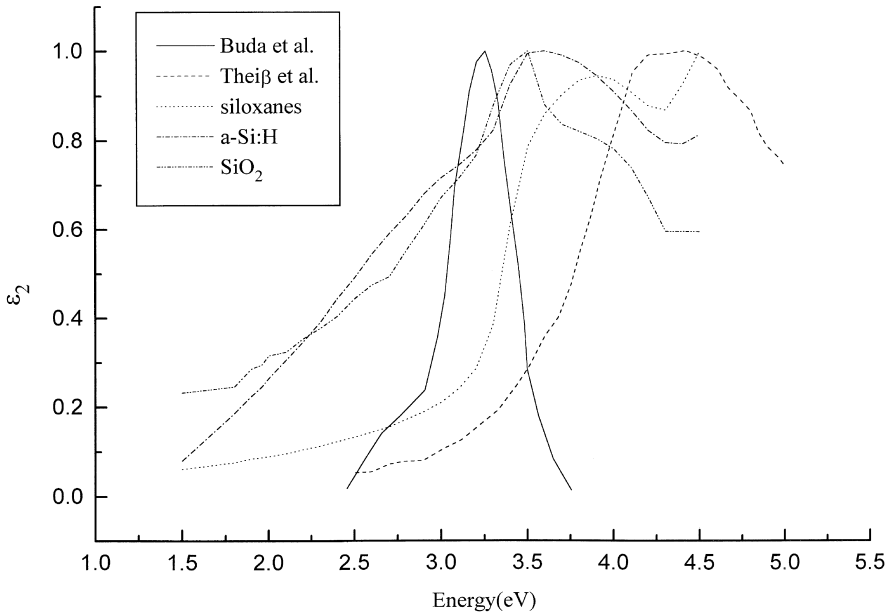

Fig. 4. Imaginary part of the normalized transverse component of the effective dielectric function of porous silicon for our approach, another mean field model [23] and a quantum wire calculation [14]. In our case we use siloxane, a-Si : H and SiO_2 on the surface with $d = 10^{-10}$ m and $P = 70\%$.

In Fig. 3 the transverse component behavior of the effective dielectric function is shown for three porosities, with a bigger $d = 10^{-9}$ m and with siloxane on the surface. In these plots we observe that for a surface size of the order of 10 atomic layers, the effect of the porosity is not so relevant in the whole interval of energy.

In Fig. 4 we compare the normalized transverse component of the effective dielectric function for a-Si : H, siloxane and SiO_2 on the surface with an effective medium calculation [23] and a first principles calculation [14]. In the three approaches a similar behavior is observed. Clearly, a surface based on a-Si : H or SiO_2 will give an enhancement in the visible range. Our approach gives some insight in understanding the role of the surface in a complex material as PS.

Fig. 5 shows the behavior of $\sqrt{\alpha h v}$ with and without surfaces $d = (10^{-10}$ m, 0 m) for a porosity of 74%, compared with an experimental result [10]. Here, without skin the observed behavior is not reproduced. The best qualitative fitting is given by the a-Si : H coverage but, unfortunately, we can only compare in a small energy region where data are available.

Another important optical property is the refractive index reported with a value of 1.33 for samples of PS with porosities of 74% [10]. In Fig. 6, the effective refractive index is shown for PS for two porosities, a thickness of $d = 10^{-10}$ m of a-Si : H and $P = (70\%, 74\%)$. The value of n is of the same order as the experimental one.
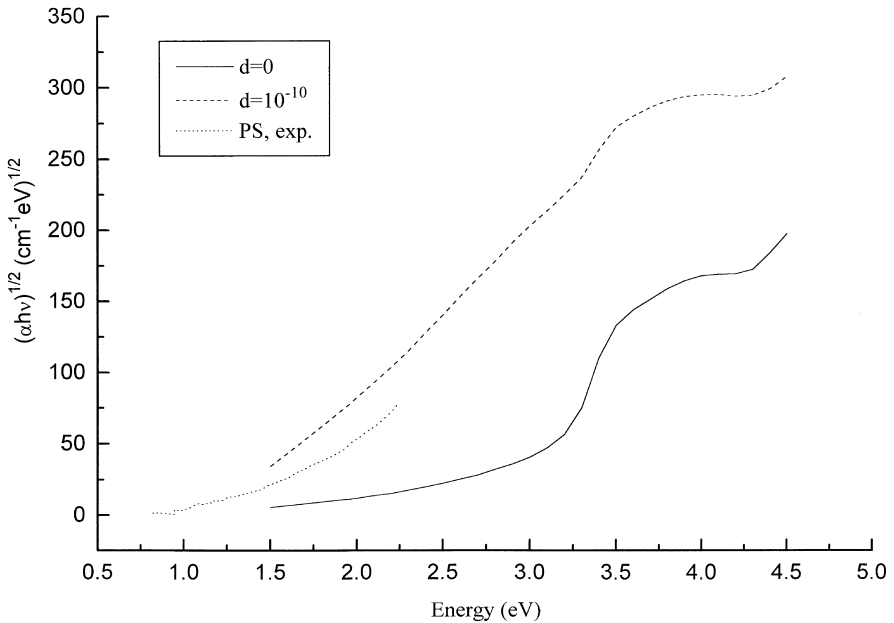

Fig. 5. Square root of the effective absorption coefficient α of porous silicon times the photon energy $h v$ vs. the photon energy, with a-Si : H on the surface, in this case the parameters are $d = 0$ m, $d = 10^{-10}$ m and $P = 74\%$ compared with experimental results [10].
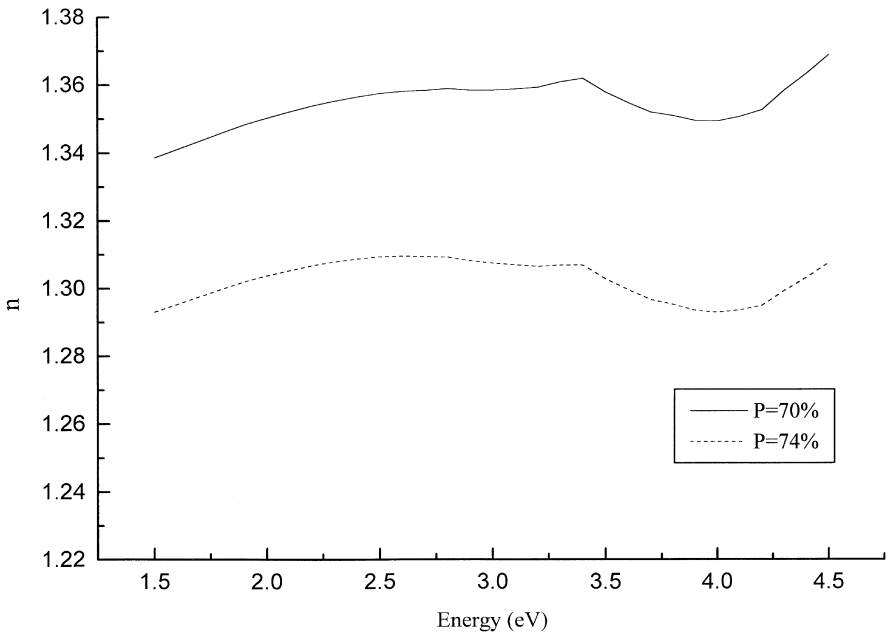
Fig. 6. Effective refractive index of our model of porous silicon with a-Si : H on the surface at porosities of 70% and 74%.

4. Conclusions

Materials with several components are difficult to characterize due to their complex structure. Under certain circumstances, from the macroscopic point of view, it is justifiable to develop a description similar to a homogeneous material that simplifies the mathematical complexity of the problem together with the physical interpretation. The VAM is an important contribution in the effective mean theories, since other similar approaches do not consider, in an easy way, the surface effects. Because the analytic results were obtained studying the volumetric and surface contribution in an independent way, it is possible to explore the role of the surface in the effective response. Our model depends on the microgeometry chosen. It has been solved for cylindrical columns but it could be calculated for other geometries such as spheres or even anisotropic shapes, although at the expense of doing it numerically.

Our results seem to indicate that the surface effects could have similar consequences to quantum confinement, at least regarding the range of relevant energies for the effective dielectric function, effective absorption coefficient and effective refractive index. The surface effects may be responsible of the change in the effective optical response energy range and not only the quantum confinement model.

In summary, we have performed a systematic analysis changing the material on the surface of a model of PS. Experimental results are strongly sample dependent and there are no results yet that are considered universal. However, comparison with new

experimental data is currently in progress. We think that undoubtedly surface effects should be taken into account in a rigorous way to understand PS.

Acknowledgements

References

[1] P.M. Fauchet, in: D.J. Lockwood (Ed.), Light Emission in Silicon, Academic Press, New York, 1996.
[2] A. Gupta, V.K. Jain, C.R. Jalwania, G.K. Singhal, O.P. Arora, P.P. Puri, R. Singh, M. Pal, V. Kumar, Semicond. Sci. Technol. 10 (1995) 698.
[3] J.P. Zheng, K.L. Jiao, W.P. Shen, W.A. Anderson, H.S. Kwok, Appl. Phys. Lett. 61 (1993) 459.
[4] L.Z. Yu, C.R. Wie, Electron. Lett. 28 (1992) 911.
[5] R. Swicher, G.L. Richmond, P.C. Sercel, J. Chem. Ed. 73 (1996) 738.
[6] G. Smestad, M. Kunst, C. Vial, Solar Energy Mater. Solar Cells 26 (1992) 277.
[7] P. Menna, G. di Francia, V. la Ferra, Solar Energy Mater. Solar Cells 37 (1995) 13.
[8] G. Bomchil, A. Halimaoui, R. Herino, Microelectron. Eng. 8 (1988) 293.
[9] L.T. Canham, Appl. Phys. Lett. 57 (1990) 1046.
[10] I. Sagnes, A. Halimaoui, G. Vincent, P.A. Badoz, Appl. Phys. Lett. 62 (1993) 1155.
[11] S.F. Chuang, S.D. Collins, R.L. Smith, Appl. Phys. Lett. 55 (1991) 1540.
[12] F. Koch, Mater. Res. Soc. Symp. Proc. 298 (1993) 319.
[13] S.M. Prokes, O.J. Glembocki, Phys. Rev. B 49 (1994) 2238.
[14] F. Buda, J. Kohnoff, M. Parrinello, Phys. Rev. Lett. 69 (1992) 1272.
[15] P.D.J. Calcott, K.J. Nash, L.T. Canham, M.J. Kane, D. Brumhead, Mater. Res. Soc. Symp. Proc. 283 (1993) 143.
[16] L. Tsybeskov, P.M. Fauchet, Appl. Phys. Lett. 64 (1994) 1983.
[17] C. Peng, K.D. Hirschman, P.M. Fauchet, J. Appl. Phys. 80 (1996) 295.
[18] J. Tagüeña, J.A. del Río, J.A. Ochoa, Solid State Commun. 90 (1994) 411.
[19] J. Tagüeña, J.A. del Río, J.A. Ochoa, Physica A 207 (1994) 163.
[20] J.A. del Río, J. Tagüeña, J.A. Ochoa, Solid State Commun. 87 (1993) 541.
[21] J. Tagueña, J.A. del Río, J.E. Lugo, J. Non-Cryst. Solids 182 (1995) 206.
[22] J.E. Lugo, J. Tagüeña, J.A. del Río, J.A. Ochoa, Mater. Res. Soc. Symp. Proc. 358 (1995) 43.
[23] W. Theiß, S. Henkel, M. Arntzen, Thin Solid Films 255 (1995) 177.
[24] W. Theiß, Thin Solid Films 276 (1996) 7.
[25] Y.H. Xie, M.S. Hybertsen, W.L. Wilson, Phys. Rev. B 49 (1994) 5386.
[26] S. Whitaker, Transport in Porous Media 1 (1986) 3.
[27] J.A. Ochoa, J.A. del Río, S. Whitaker, Chem. Eng. Sci. 48 (1993) 2061.
[28] J.A. Ochoa, S. Whitaker, P. Stroeve, Chem. Eng. Sci. 49 (1994) 709.
[29] H.-C. Chang, Chem. Eng. Commun. 15 (1982) 83.
[30] J.E. Lugo, Propiedades Efectivas del Silicio Poroso Optoluminiscente, M.Sc. Thesis (1995).
[31] G.E. Jellison, Optical Mater. 1 (1992) 41.
[32] M. Fried, T. Lohner, J. Appl. Phys. 71 (1992) 5260.
[33] M. Rosenbauer, M. Kelly, Max Planck Institut Stutgart, private communication, 1994.
[34] S. Boultadakis, S. Logothetidis, A. Papadopoulos, N. Vouroutzis, Ph. Zorba, J. Appl. Phys. 78 (1995) 4164.
[35] N. Koshida, Appl. Phys. Lett. 63 (1993) 2774.